Lasers in Manufacturing Conference 2017

Influence of oscillation parameter on melt pool geometry and hot cracking susceptibility during laser beam welding of high strength steels

Vincent Mann[a,*], Matthias Holzer[a], Konstantin Hofmann[a], Andreas Korbacher[a, b], Stephan Roth [a, c], Peter Weidinger[d], Michael Schmidt[a, b, c]

[a] *Bayerisches Laserzentrum GmbH (blz), Konrad-Zuse-Straße 2-6, 91052 Erlangen, Germany*
[b] *Institute of Photonic Technologies (LPT), Friedrich-Alexander-Universität Erlangen-Nürnberg, Konrad-Zuse-Straße 3-5, 91052 Erlangen, Germany*
[c] *Erlangen Graduate School in Advanced Optical Technologies (SAOT), Paul Gordan Straße 6, 91052 Erlangen, Germany*
[d] *Friedrich-Alexander-University Erlangen-Nuremberg, Department of Materials Science and Engineering Institute of General Material Properties (WW1), Martensstraße 5, 91058 Erlangen, Germany*

Abstract

As the alloying content of high strength steels is increased in comparison to mild steels, the susceptibility for hot cracking is raised simultaneously due to the larger solidification range of the materials. Besides the alloying composition, hot cracking is also influenced by thermal strains and the temperature field within the welding process, which can hardly be manipulated in conventional laser beam welding.
Here laser beam welding with beam oscillation offers new possibilities to influence the temperature field as well as the resulting thermal strains and also the solidification conditions. Thus within this paper the influence of oscillation parameters on melt pool geometry and hot cracking susceptibility during laser beam welding of high strength steels is investigated. The experimental results show, that solidification conditions are influenced and hot cracking susceptibility is decreased by applying a superimposed beam oscillation during the welding process.

Keywords: Marco Processing; Joining; Welding

* Corresponding author. Tel.: +49 (0)9131/9779016; fax: +49 (0)9131/9779011.
E-mail address: v.mann@blz.org

1. Introduction

Nowadays the individual mobility is undergoing a fundamental change, since the supplies for fossil fuels are dwindling and thus costs for energy are increasing. Besides this the strictly increasing standards for CO_2 and NO_X emissions of vehicles force automotive manufactures to develop new vehicle concepts. Apart from new drive types like electric engines, lightweight construction is still of high importance, e.g. to ensure a sufficient range of electric cars. In this context high strength steels are often used for car body manufacturing and safety and interior parts due to their advantageous mechanical properties and their high availability and processability. In contrast to the manufacturing process of mild steels, the production procedure of high strength steels is characterized by the exact control of temperature, cooling rate, holding time and the degree of deformation during the rolling process of the slabs. These parameters are the basis for high strength and ductility of the final products. This manufacturing method is called thermomechanical rolling and provides a fine grained structure of the material which ensures the desired properties. Weißbach 2007 Moreover high strength steels have a higher content of alloying elements, e.g. titanium, niobium, silicon, boron and manganese, which are required for further hardening mechanisms like solid solution hardening. Roos et al. 2015 Thus, in contrast to pure metals like iron, aluminum or copper, these alloys have no melting point at a certain temperature but a temperature interval of liquation and solidification, which is expanded with an increasing content of alloying elements.

In welding of those alloys, the high content of alloying elements leads to an elevated susceptibility for welding defects. Typical welding defects which are caused by an increased content of alloying elements are hot cracks. These defects are formed within the solidification temperature range of the alloys during the cooling phase, when liquid as well as solid material is present at the same time. DVS 1996 In order to prevent the formation of hot cracks, often a change of the alloying composition within the weld seam is induced by the use of filler materials like high silicon-content aluminum alloys for welding of high strength aluminum materials. Seefeld and Schultz 2013 However this method is undesired for laser beam welding of high strength steels due to the higher effort for the supply of filler materials. Furthermore the possibility for remote welding applications is significantly restricted for using filler wire. Therefore within this paper an approach for decreasing hot cracking susceptibility in laser beam welding of high strength steels without the use of filler material is presented. Here a superimposed beam oscillation is used to modify the temperature field as well as the solidification conditions, in detail the direction of crystallization during cooling phase of the welding process. In this context the influence of the different welding and oscillation parameters on the resulting weld pool geometry on the surface is determined by means high-speed imaging.

2. State of the art

2.1. Formation of hot cracks

Hot cracks appear as a result of a critical combination of thermomechanical load which is induced by the shrinking procedure during the cooling phase in welding and casting processes and the appearance of low melting phases during a cellular or dendritic crystal growth. Cross 2005 According to Radaj 1988 there are different stresses and strains during the welding process, which are mainly affected by the heat input per unit length and the location of the observed position in relation to the melt pool. As the material in front of the melt pool is heated up by heat conduction, it expands and consequently a zone of compressive stresses is generated in front of the melt pool. As soon as the melt pool passes this zone, these stresses are relieved by deformation of the molten material and root sagging and weld reinforcement are formed. Subsequently the cooling phase of the material starts after the energy source has passed the observed region. During this

phase the material cools down, solidifies and contracts due to the thermal shrinking processes. Radaj 1988 In this phase hot cracks appear, if strains exceed a material specific deformation limit P. Prokhorov et al. 1968 In this case the low melting liquid phases among the dendritic network are inhibiting a coalescence of the dendrites and thus the transfer or compensation of the strains through or within the weld seam. As in this state the material is almost completely solidified and there is a certain distance to the melt pool, shrinking of the material cannot be replenished by melt from the melt pool anymore. Borland 1960 and Feurer 1977 In this case the pressure within the melt drops locally below the cavitation pressure of the material and cavities are formed. These cavities act as a starting point for the initiation of hot cracks. Rappaz et al. 1999

Therefore the type and direction of the crystal growth during the solidification of the material within the welding process is of importance for the ability of the crystal network to compensate and transfer strains and to ensure the transport of the melt in order to refill cavities and compensate shrinking. For this reason Katayama 2000 investigated the influence of welding parameters on the type and direction of the resulting crystal structure within the weld seam. As the direction of crystal growth depends on the temperature gradient, an influence of welding velocity and melt pool geometry on the crystal structure and the formation of hot cracks as shown in Fig. 1 was identified. Here an increase of the welding velocities results at first in a change of the growing direction of the dendrites towards the middle of the weld seam. As a consequence low melting phases are concentrated in middle of the weld seam and hot cracking susceptibility rises. A further increase of welding velocity leads to equiaxed dendritic crystal growth in middle of the weld seam and an equal distribution of the low meting phased which decreases the hot cracking susceptibility. Katayama 2000

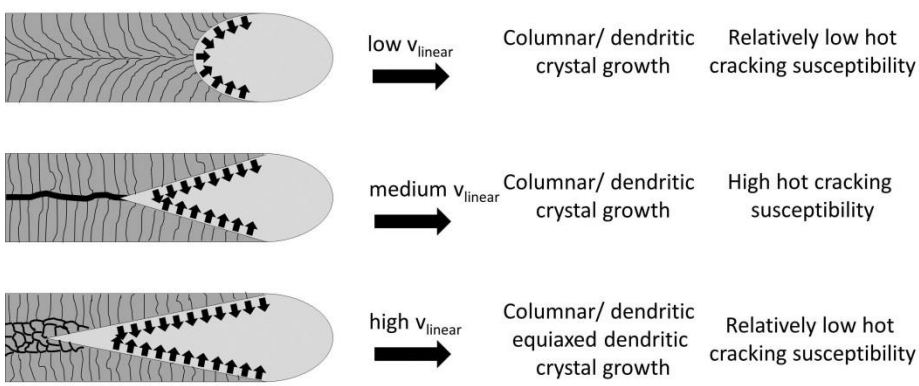

Fig. 1. Relation of welding velocity and weld pool geometry to direction of primary crystal growth and hot cracking susceptibility according to Katayama 2000

According to these results the temperature gradient, the geometry of the melt pool and the cooling conditions are important factors for the formation of hot cracks. For this reasons another method besides changing the welding velocity for varying the energy input may be beneficial for an manipulation of melt pool shape and cooling conditions.

2.2. Welding with superimposed beam oscillation

The latest developments in high brilliant laser sources with high output powers in the kilowatt range and the availability of systems for fast deflection of laser beams enable welding processes with a fast superimposed beam oscillation Schweier 2015. For this purpose often circular, sinusoidal, zig-zag and

lemniscates are used as oscillation figures. In case of lower laser powers several transmissive and reflective devices for the deflection of the beam can be employed. If the process requires laser powers in the multi kilowatt range and a high flexibility regarding welding contours, galvanometer scanners are a suitable choice. Schmitt 2012 For laser beam welding processes a superimposed beam oscillation is used in combination with filler wires to increase the bridgeable gap width. Here investigations showed that a gap width of 1 mm was bridged by using a laser beam with a focal diameter of 19 µm and a wire feeding speed of 3.5 m/min by applying a superimposed zig-zag beam oscillation with an amplitude of 0.7 mm. Seefeld and Scholtz 2013 Furthermore a zig-zag oscillation was beneficial for improving the surface quality in laser beam welding of aluminum. Here oscillation frequencies of 200 Hz and welding speeds of less than 2 m/min result in smooth surfaces of the weld seams. Schultz 2014 Besides this, Schmitt 2012 investigates the effect of a circular beam oscillation on the melt pool dynamics during laser beam welding of dissimilar material combinations in lap joint configuration. For this purpose the joining partners were X5CrNi18-10 as upper joining partner and pure iron as lower joining partner. The subsequent determination of the chromium content within the weld seam offers the possibility for conclusions on the melt pool dynamics. Another field of application for laser beam welding with beam oscillation is presented by Fetzer et al. 2016. The authors investigated welding of copper aluminum connections in lap joint configuration. Here a mixture of molten copper and aluminum and the subsequent formation of intermetallic phases have to be suppressed, as they decrease the electrical conductivity and the mechanical properties of the connections. For this reason beam oscillation was used to modify the melt pool geometry in order to produce weld seams with a large width, a shallow depth and a large cross-section between the joining partners. In particular the influence of the oscillation figure and the amplitude were investigated. Fetzer et al. 2016. Thus beam oscillation seems to be an adequate method for modelling the melt pool shape. Nevertheless there are no investigations on laser beam welding with a superimposed fast beam oscillation with the intention to reduce the hot cracking susceptibility during the welding of high strength steels.

3. Experimental setup

All welding experiments were carried out with a disk laser with a maximum output power of 6 kW, a wavelength (λ_L) of 1,030 nm, the focal plane on the surface of the sheets and a beam parameter product of 4 mm x mrad. The laser radiation was guided by an optical fiber with a core diameter of 100 µm to a Trumpf 2D-scanner optic with a collimation length of 150 mm and a focusing length of 255 mm leading to a focal diameter (d_f) of 170 µm. The movement of the laser beam was realized solely by the scanner optics and no additional axle was employed. For all experiments a circular oscillation pattern was used. For an observation of the welding process and the melt pool, a high speed camera was positioned at a lateral position working with an exposure time (t) of 1 µs and a recording frequency (f_{HSC}) of 30 kHz. In order to eliminate process radiation a bandpass filter was place in front of the camera objective. On the opposite side pulsed illumination laser was installed to improve the brightness of the videos. Here the illumination and observation wavelength (λ_{IL}) was chosen to be 808±1 nm and the pulse duration was 250 ns. The specimens are clamped firmly within a clamping device at their wider edge by a screw. The complete experimental setup is shown in Fig. 2.

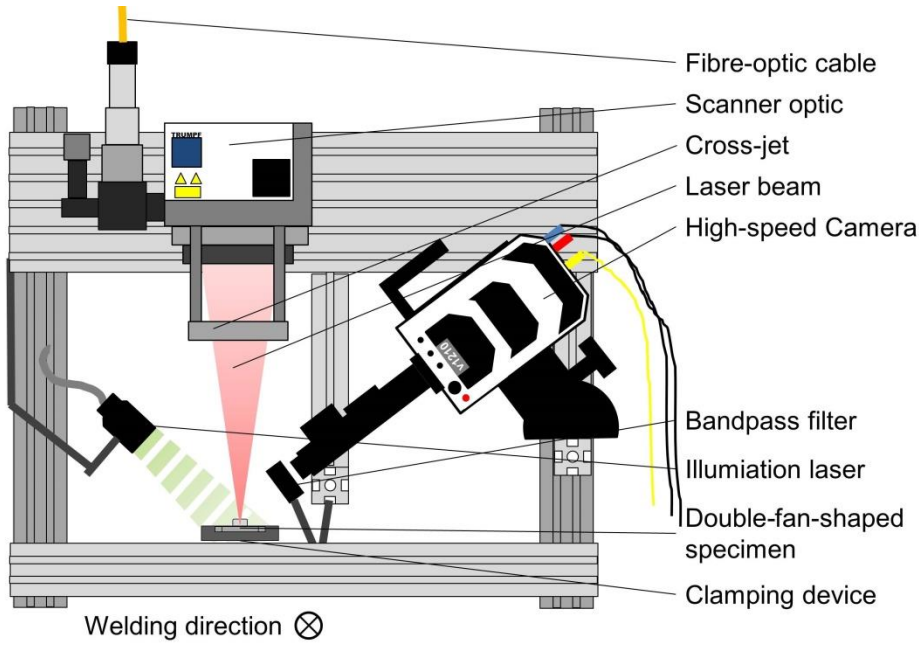

Fig. 2. Experimental setup for self-restrained hot cracking tests

The welding and oscillation parameters which were varied during the experiments are documented in Table 1. All welding experiments were carried out as bead-on-plate welds.

Table 1. Welding and oscillation parameters used for the experiments

Parameter	Symbol	Tested range	Unit
Laser power	P_L	2.25 – 3.5	kW
Linear welding velocity	v_L	10 – 60	mm/s
Figure overlap	O	60 – 80	%
Oscillation frequency	f	19 – 115	Hz
Oscillation amplitude	A	0.5 – 1	mm

The geometrical dimensions of the self-restrained hot cracking specimens as well as the area of interest observed by the high-speed camera during the process are illustrated in Fig. 3. The specimens are developed on the basis of the Fan-shaped-cracking test invented by Matsuda and Nakata 1982 and have another trapeze at the narrower edge. Due to that, a higher energy for crack initiation is necessary, as the starting point of the hot crack appears at a certain distance to the starting point of the weld seam after passing the waist of the specimen. Furthermore the middle of the weld seam was positioned at a constant distance (a) of 1.5 mm from the symmetry plane of the specimens, whereas the weld seams have a length of 100 mm, which means 50 mm to each side of the waist of the specimen. The samples are produced by laser beam cutting of high-strength-low-alloy steel with an yield strength of at least 700 MPa from sheets with a thickness of 1.8 ± 0.05 mm.

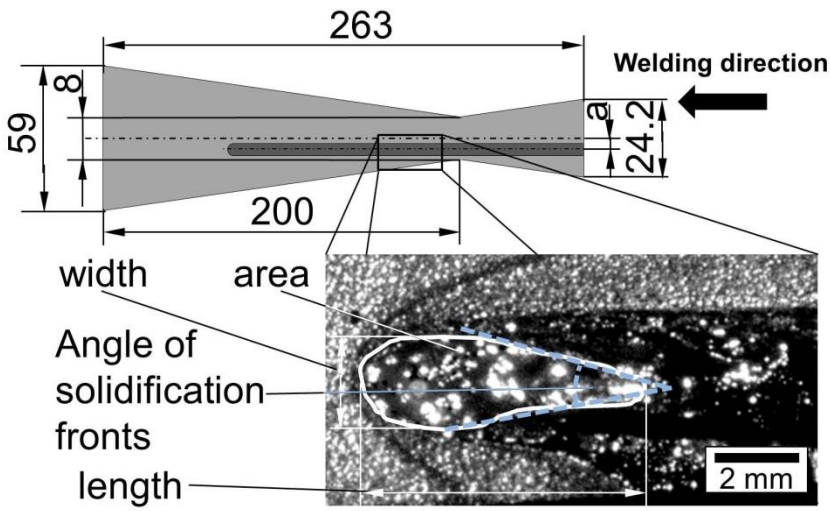

Fig. 3. Geometry of the Double-fan-shaped specimens and exemplary high-speed image for the determination of the weld pool dimensions

4. Results and Discussion

4.1. Process characteristics

In the following chapter the results of the experiments on welding of high steels with a superimposed beam oscillation are presented and discussed by means of a subsequent evaluation of several oscillation parameters and their influence on the melt pool geometry. As self-restrained hot cracking tests were used for the experiments, the width of the specimens changes along the weld seam due to the different conditions for heat conduction. Furthermore the stiffness of the specimens varies along the weld seam depending on the local width. For this reason for a critical set of welding parameters hot cracks appear after the welding process has passed the waist of the samples. As shown in Fig. 1 the melt pool geometry influences the formation of hot cracks. Thus characteristic values of the melt pool were determined by means of high-speed videos. Fig. 4 shows the progress of the length, width and area of the melt pool surface as well as the angle of the solidification fronts for three different time steps. At the first time step the melt pool has passed the waist of the specimens, whereas the melt pool has moved 4 mm respectively 8 mm in welding direction at the second and third time step. As heat conduction increases with increasing width of the specimens after the melt pool passes the waist, the length and area of the melt pool are decreasing. On the other hand the weld seam width remained unchanged due to the constant oscillation amplitude. As a result the angle of solidification fronts increases at the same time. For the discussed set of parameters hot cracks appear in 66% of the specimen.

4.2. Influence of the laser power

For the determination of the influence of different welding and oscillation parameters, the average values derived of the three different time steps shown in Fig. 4 and two high-speed videos are compared as depicted in Fig. 5. Due to that the standard deviation is higher compared to Fig. 4. In particular Fig. 5 shows

the influence of laser power on the resulting melt pool geometry. For higher laser power the length and area of the melt pool are increasing, due to the higher energy input, while the width remains constant. According to this the angle of solidification fronts decreases for higher laser powers. As 100% of the tested specimens show hot cracks at the highest laser power, the determined melt pool geometry can be identified to be disadvantageous regarding the hot cracking susceptibility during the process.

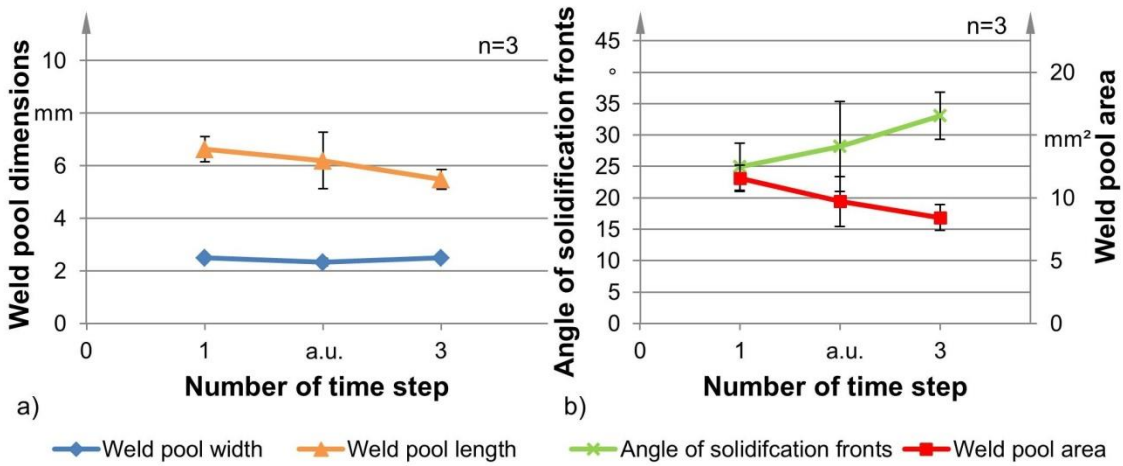

Fig. 4. Weld pool dimensions next to the waist of the specimens for three different process times (a) width and length of the weld pool; (b) angle of solidification fronts and area of the weld pool; both: Welding parameters: P_L: 2.5 kW; v_L: 10 mm/s; Pattern: circle; O: 60%; A: 0.5 mm; f: 30 Hz; a: 1,5 mm; d_f: 170 µm; λ_L: 1,030 nm; Material: High-strength-low-alloy steel; d: 1,8 ± 0,05 mm; Double-Fan-Shaped specimens; recording parameters: t: 1 µs; f_{HSC}: 30 kHz; λ_{IL}: 808 ± 1 nm

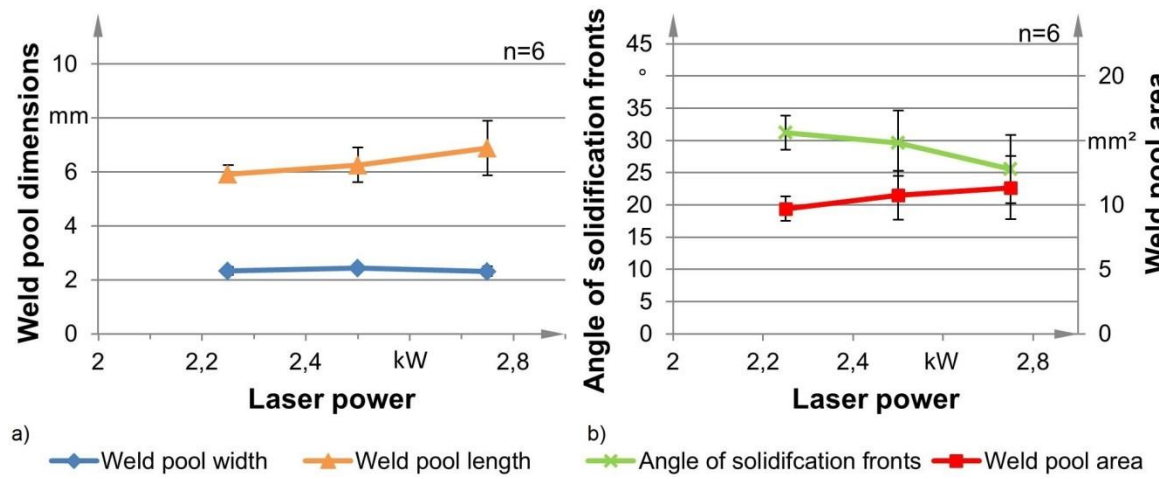

Fig. 5. Weld pool dimensions next to the waist of the specimens for three different laser powers (a) width and length of the weld pool; (b) angle of solidification fronts and area of the weld pool; both: Welding parameters: P_L: 2.25 kW, 2.50 kW, 2.75 kW; v_L: 10 mm/s; Pattern: circle; O: 70%; A: 0.5 mm; f: 39 Hz; a: 1,5 mm; d_f: 170 µm; λ_L: 1,030 nm; Material: High-strength-low-alloy steel; d: 1,8 ± 0,05 mm; Double-fan-shaped specimens; recording parameters: t: 1 µs; f_{HSC}: 30 kHz; λ_{IL}: 808 ± 1 nm

4.3. Influence of the figure overlap

The figure overlap during welding with beam oscillation as defined in Schweier 2015 is calculated by dividing the overlapping length of two consecutive oscillation figures by the expansion length of one oscillation figure in welding direction. For constant oscillation amplitudes the figure overlap directly determines the oscillation frequency. The influence of different figure overlaps on the melt pool geometry at the surface is depicted in Fig. 6. As for higher laser powers, the area and length of the melt pool is increasing with increasing figure overlaps, while the width stays constant. This can be explained by a higher percentage of directly irradiated material at higher figure overlaps. Therefore there is a higher coupling efficiency and a lower proportion of transmitted energy. Departing from Fig. 5 no clear trend for the development of the angle of solidification fronts can be identified. While there is an increase for a figure overlap of 70% in comparison to 60%, the angle drops to almost the initial value for a figure overlap of 80% again. This corresponds to the results of the hot cracking tests, since for figure overlaps of 60% as well as 80%, 66% of the specimens show hot cracks, while no hot cracks were found for a figure overlap of 70%. As a conclusion for the investigated set of parameters a value of the angle of solidification fronts of 30° was identified to be a lower material-specific limit for the formation of hot cracks.

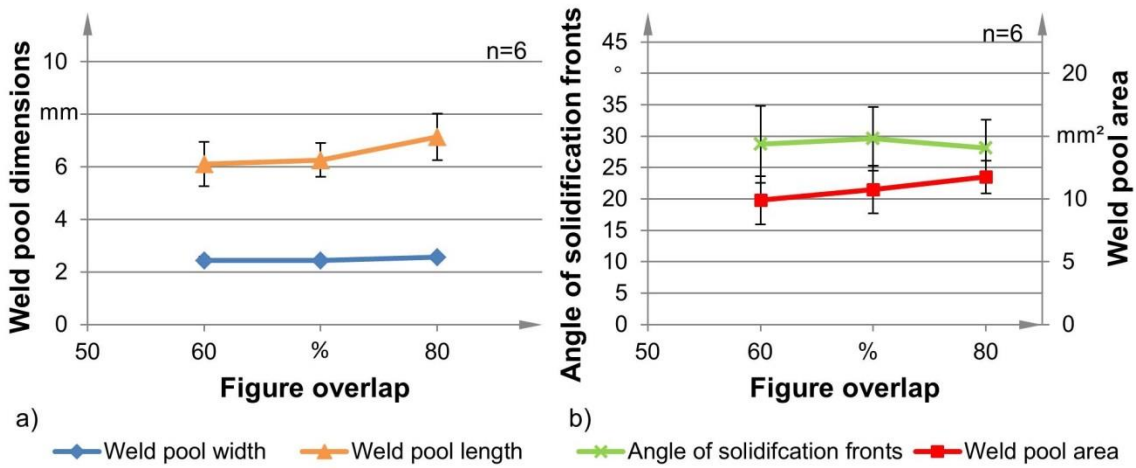

Fig. 6. Weld pool dimensions next to the waist of the specimens for three different figure overlaps (a) width and length of the weld pool; (b) angle of solidification fronts and area of the weld pool; both: Welding parameters: P_L: 2.5 kW; v_L: 10 mm/s; Pattern: circle; O: 60%, 70%, 80%; A: 0.5 mm; f: 30 Hz, 39 Hz, 55 Hz; a: 1,5 mm; d_f: 170 µm; λ_L: 1,030 nm; Material: High-strength-low-alloy steel; d: 1,8 ± 0,05 mm; Double-fan-shaped specimens; recording parameters: t: 1 µs; f_{HSC}: 30 kHz; λ_{IL}: 808 ± 1 nm

4.4. Influence of the welding velocity

Since the linear welding velocity has a significant influence on the formation of hot cracks in conventional welding (Fig. 1), this parameter was also investigated during the experiments. Hence Fig. 7 shows the effect of linear welding velocity on the resulting melt pool geometry. Here an increase of linear welding velocity results in a small decrease of width and length of the melt pool. Moreover a significant reduction of the melt pool area due to the lower energy input per unit length is visible, while the angle of solidification fronts stays at an almost constant level of about 21°. As this value is below the material-specific level of 30° identified in Fig. 6, it can be assumed that hot cracks are detectable in each self-restrained hot cracking test specimen. In fact hot cracks were only detected in case of the lower linear welding velocity for all investigated samples.

This leads to the conclusion that the angle of solidification fronts is not a single dominating factor for the formation of hot cracks. Since the energy input per unit length is significantly reduced by the higher welding velocity, also the area of the melt pool decreases. This decrease is coupled with a reduction of the appearing strains within the welding process as explained in the state of the art. Simultaneously the hot cracking susceptibility during the process is reduced. According to these results a critical and material specific combination of a small angle of solidification fronts and certain size of the melt pool is required to induce the formation of hot cracks in laser beam welding with beam oscillation.

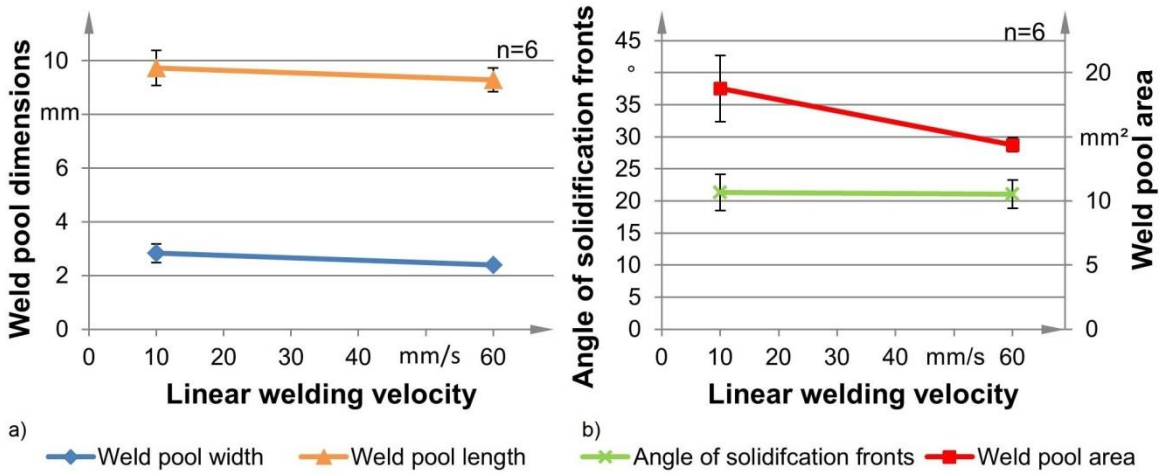

Fig. 7. Weld pool dimensions next to the waist of the specimens for two different linear welding velocities (a) width and length of the weld pool; (b) angle of solidification fronts and area of the weld pool; both: Welding parameters: P_L: 3.5 kW; v_L: 10 mm/s, 60 mm/s; Pattern: circle; O: 70%; A: 1 mm; f: 19 Hz, 115 Hz; a: 1,5 mm; d_f: 170 µm; λ_L: 1,030 nm; Material: High-strength-low-alloy steel; d: 1,8 ± 0,05 mm; Double-fan-shaped specimens; recording parameters: t: 1 µs; f_{HSC}: 30 kHz; λ_{IL}: 808 ± 1 nm

4.5. Influence of the oscillation amplitude

Another main oscillation parameter, whose effect on the melt pool geometry is illustrated in Fig. 8, is the oscillation amplitude. Due to the higher width of the irradiated zone, the energy density within the welding process decreases. For this reason there is only a small expansion of length and width of the melt pool. Contrary to these results the area of melt pool and the angle of solidification fronts show a higher increase for the higher oscillation amplitude which is mainly caused by an extension of the leading part of the melt pool. This region is characterized by almost parallel melt pool boundaries on each side of the melt pool. Regarding the results of self-restrained hot cracking tests all specimens show hot cracks for the smaller oscillation amplitude. A comparison with the results depicted in Fig. 5 and Fig. 6 shows a larger area of the melt pool in Fig. 8. For this reason there is a higher thermal expansion of the samples, which causes an increase of the tension strains occurring behind the melt pool during the cooling process of tested specimens. Hence even for angles of the solidification fronts above 30° hot cracks appear in 66% of the self-restrained hot cracking tests for an oscillation amplitude of 2 mm.

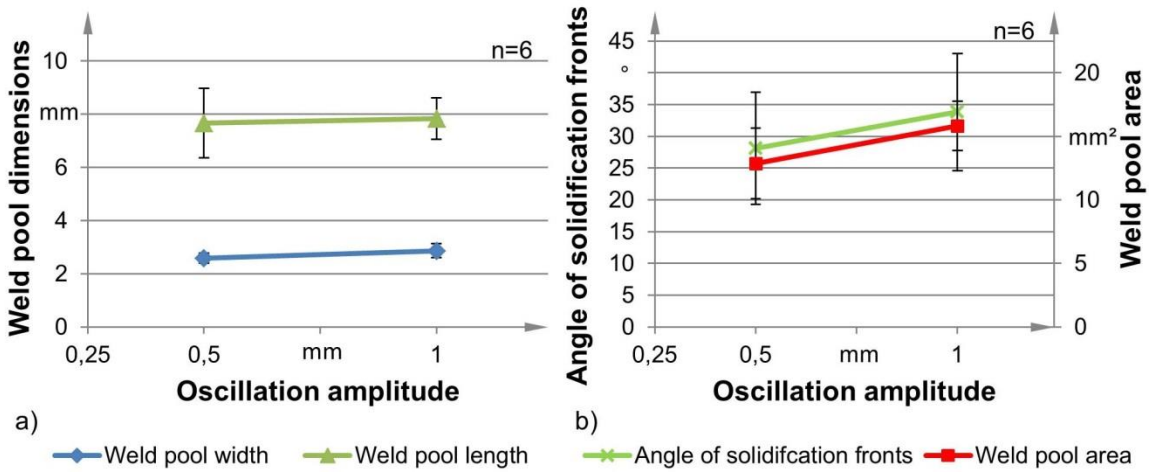

Fig. 8. Weld pool dimensions next to the waist of the specimens for two different oscillation amplitudes (a) width and length of the weld pool; (b) angle of solidification fronts and area of the weld pool; both: Welding parameters: P_L: 3 kW; v_L: 10 mm/s; Pattern: circle; O: 60%; A: 0.5 mm, 1 mm; f: 15 Hz, 30 Hz; a: 1,5 mm; d_f: 170 µm; λ_L: 1,030 nm; Material: High-strength-low-alloy steel; d: 1,8 ± 0,05 mm; Double-fan-shaped specimens; recording parameters: t: 1 µs; f_{HSC}: 30 kHz; λ_{IL}: 808 ± 1 nm

5. Conclusion and outlook

This paper shows the results of the experimental investigation of the influence of oscillation and welding parameters on the melt pool geometry and hot cracking susceptibility in laser beam welding of high strength steels. For this purpose the width, length and area of melt pool as well as the angle of solidification fronts were determined by means of high-speed videos. As a result critical material-specific combinations of the melt pool area on the surface and the angle of solidification fronts are identified to facilitate the formation of hot cracks. In particular a reduction of the laser power as well as an increase of linear welding velocity and oscillation amplitude are determined to be beneficial to reduce hot cracking susceptibility during the process, whereas no clear trend can be identified in case of figure overlap or oscillation frequency, respectively. In further experiments the effect of oscillation parameters on the melt pool geometry and hot cracking susceptibility will be further investigated in order to get more stringent results with regard to critical values of the melt pool area and angles of the solidification fronts. Moreover other materials and oscillation figures will be examined. In addition other amplitudes, linear welding velocities, focal diameters and oscillation frequencies will be regarded.

Acknowledgements

The presented results are accomplished with the project SQLaP which is funded by the Bavarian Research Foundation. The authors want to thank the Foundation and the Bavarian State Government for funding.

References

Borland, J., 1960. Generalized theory of super-solidus cracking in welds and castings, British Welding Journal 7, p. 508.

Cross, C. E., 2005. On the Origin of Weld Solidification Cracking, Hot cracking phenomena in welds (Böllinghaus, T., Herold, H.), Springer Verlag, Berlin, Heidelberg, p. 3.

DVS technical bulletin 1004-1, 1996. Heißrissprüfverfahren – Grundlagen. Deutscher Verband für Schweißtechnik. Düsseldorf

Fetzer, F., Jarwitz, M., Stritt, P., Weber, R. Graf, T., 2016. Fine-tuned remote laser welding of aluminum to copper with local beam oscillation. Physics Procedia 83, 9th International Conference on Photonic Technologies, Proceedings of the LANE 2016, p. 455.

Feurer, U., 1977. Influence of alloy composition and solidification conditions on dendrite arm spacing,feeding and hot tearing properties of aluminium alloys. Proceedings International Symposium on Engineering Alloys, Delft, p. 131.

Katayama, S., 2000. Solidification phenomena of weld metals(1st report). Characteristic solidification morphologies, microstructures and solidification theory. Welding International, p. 939.

Matsuda, F., Nakata, K., 1982. A New Test Specimen fpr Self-Restraint Solidification Crack Susceptibility Test of Electron-Beam Welding Bead, Welding Research Institute of Osaka University, Osaka.

Prokhorov, N.N; Jakuschin, B.F.; Prochorow, N.N, 1968. Theorie und Verfahren zum Bestimmen der technologischen Festigkeit von Metallen während des Kristallisationsprozesses beim Schweißen. Schweißtechnik 18, VEB Verlag, Berlin. Number 1, p. 8

Radaj, D., 1988. Wärmewirkungen des Schweißens – Temperaturfeld, Eigenspannungen, Verzug. 1st edition. Springer Verlag, Berlin.

Rappaz, M., Drezet, J.-M., Gremaud, M. 1999. A new hot-tearing criterion, Metallugical and Materials Transactions, Volume 30 A, p. 449

Roos,E., Maile,K., 2015. Werkstoffkunde für Ingenieure – Grundlagen, Anwendung, Prüfung. 5th edition, Sringer Verlag, Berlin, Heidelberg

Schmitt, F., 2012. Laserstrahl-Mikroschweißen mit Strahlquellen hoher Brillanz und örtlicher Leistungsmodulation. Dissertaion at the RWTH University Aachen.

Schultz, V., Seefeld, T., Vollertsen, F., Gap bridging ability in laser beam welding of thin aluminum sheets. 8th International Conference on Photonic Technologies, Proceedings of the LANE 2014.

Schweier, M., 2015. Simulative und experimentelle Untersuchungen zum Laserschweißen mit Strahloszillation. Dissertation at the Technical University of Munich.

Seefeld, T., Schultz, V., 2013. New developments in filler wire assisted laser joining of aluminum. 6th International Congress on Laser Advanced Materials Processing – Proceedings of the LAMP 2013.

Weißbach, W., 2007. Werkstoffkunde – Strukturen, Eigenschaften, Prüfung. 16th edition, Viewegs Fachbücher der Technik, Wiesbaden